Applied Acoustics 174 (2021) 107790

Contents lists available at ScienceDirect

Applied Acoustics

journal homepage: www.elsevier.com/locate/apacoust

Acoustic investigation of high-sensitivity spherical leak detector for liquid-filled pipelines

Huang Xinjing, Li Zan, Li Jian *, Feng Hao, Zhang Yu, Chen Shili

State Key Laboratory of Precision Measuring Technology and Instruments, Tianjin University, Tianjin 300072, China
Binhai International Advanced Structural Integrity Research Centre, Tianjin 300072, China

ARTICLE INFO

Article history:
Received 17 August 2020
Accepted 10 November 2020
Available online 29 November 2020

Keywords:
Spherical detector
Leak detection
Pipeline
Acoustic sensor
Internal inspection

ABSTRACT

Inner spherical detectors (SDs) can approach the leak point of a liquid-filled pipeline from the inside, and therefore potentially have very high leak detection sensitivity. This paper demonstrates the SD's high sensitivity of detecting tiny, continuous leak, from the perspective of systematic acoustic sensing via finite element simulations and experiments. The SD forms a closed air cavity which may acoustically resonate and thus amplify the transmitted sound induced by leaks. The original leak induced sound is broadband and can cover several meters, so the acoustically resonant, narrow-band and movable SD can always capture the leak signal while rolling forward in the pipeline. The SD has multiple acoustic modes, but the first one is the most stable and hardly susceptible to slight changes of the air cavity. The SD has acoustic directivity, but this does not hinder leak detection, because the SD will roll over several cycles while passing by the leak point. Characteristic frequencies of the SD are determined by the air cavity and independent of shell materials; nevertheless, the resin SD has better sound permeability than the aluminum SD, and therefore has higher sensitivity. Finally, the aluminum SD is used to detect the leak in a water-filled pipeline and achieves a high sensitivity up to 0.164 L/min.

© 2020 Elsevier Ltd. All rights reserved.

1. Introduction

Pipelines are the most economical and efficient way of continuously transporting liquid resources such as crude oil, petroleum products, water, and natural gas. As pipelines are being widely utilized, on one hand, the number of pipelines is increasing year by year, on the other hand, pipelines are seriously aging and corroded, and leakage accidents often occur. Once the pipeline leaks, it will cause serious environmental pollution, economic losses and casualties. Therefore, it is necessary to detect pipeline leaks, especially early small leaks.

Leak detection techniques for pipelines in service may be classified as software-based methods and hardware-based methods [1–3]. Software-based methods measure internal pipeline parameters, including pressure, flow rate and temperature, and use various types of computer software to analyze and detect leaks in pipeline systems. Software-based methods cannot detect tiny leak and cannot locate the leak point. Hardware-based methods utilize various sensing equipment/devices to detect and locate the leak from either outside or inside of the pipeline via sensing the leaked chemical substances, induced pressure change, sound, vibration, and temperature change. Among these methods, the acoustic leak detection method is the most widely used.

Sudden large leaks can generate negative pressure wave (NPW, a kind of infrasound wave, belongs to acoustic method) in the pipeline and travel a long distance along the pipeline to both ends; the NPW is detected by the pressure transmitters at both ends, and the leak is detected and located by using the time difference of NPW arrivals [4,5]. The NPW based method cannot detect continuous leaks and small leaks. When a pressurized pipeline leaks, turbulence near the leak aperture triggers acoustic signals, which propagate upstream and downstream along both the pipeline wall and the liquid column inside [6–8], and are finally captured by acoustic emission sensors, accelerometers or hydrophones installed on the pipeline.

The advantage of non-NPW, acoustic leak detection methods is that they can detect continuous leaks, while its disadvantage is that the monitored pipeline is very short, because the sound wave attenuates quickly during the process of propagation along the pipeline and the propagation distance is very short [9,10]. It is impractical to densely install sound sensors along the pipeline. One alternative method to solve this problem is to use distributed optical fiber to monitor the vibration caused by leaks (as well as

* Corresponding author.
E-mail address: tjupipe@tju.edu.cn (J. Li).

https://doi.org/10.1016/j.apacoust.2020.107790
0003-682X/© 2020 Elsevier Ltd. All rights reserved.

temperature change caused by leaked liquid). However, the optical fiber needs to be laid at the same time when the pipeline is laid, and many old pipelines with a high risk of leak are not accompanied by optic fibers. In addition, the optical fiber is not sensitive to leak occurring on the opposite side of the pipeline. Another method is to use an inner spherical detector (SD) to carry a sound sensor and move close to the leak point to listen to the leak induced sound from the inside of the pipeline [11–13]. The diameter of the SD is smaller than that of the pipeline, so it can roll freely under the push of the fluid in the pipeline. The SD can detect leaks at every point of the entire pipeline. The blocking risk of the SD is very low and the noise is also very low. The SD can be frequently launched to achieve quasi real-time detection.

The principle of the SD to detect pipeline leak is shown in Fig. 1. The SD is put into the pipeline from one end and rolls forward under the drive of the liquid in the pipeline. When the pipeline leaks, a broadband leak sound will be produced at the leaking point and propagates a certain distance to both sides. When the SD passes through the leak point, the leak sound can be detected and used to determine the occurrence of the leak. The SD is a sealed spherical shell with an air cavity that has hard acoustic boundary conditions. The air cavity resonates under the excitation of external leak sound. A sound logger is sealed in the air cavity to sense the sound pressure transmitted from the external water into the air cavity. The sealed sphere can not only produce a closed air cavity that may acoustically resonate but also waterproof and protect the internal electronic devices. The SD is a narrow-band, movable detection method.

Previous researches on the SD only involve structural design, electronic component integration and signal processing, and have not investigated the sound sensing characteristics of the SD taking into account the detection principle and working conditions in order to improve the sensitivity of leak detection. This paper investigates frequency spectrum characteristics and spatial distribution characteristics of the sound inside the pipeline caused by continuous leaks via finite element simulations and experiments, so as to match the narrow-band, movable SD for leak detection. Then it studies the acoustic sensing characteristics of the SD and their influencing factors via simulations and experiments, and discusses the impacts of these acoustic sensing characteristics on the leak detection performances of the SD in the pipeline. Finally, leak detection test on a liquid-filled pipeline is carried out to demonstrate the SD's high sensitivity of leak detection, and key points that need to be considered when designing the SD for field applications are also discussed.

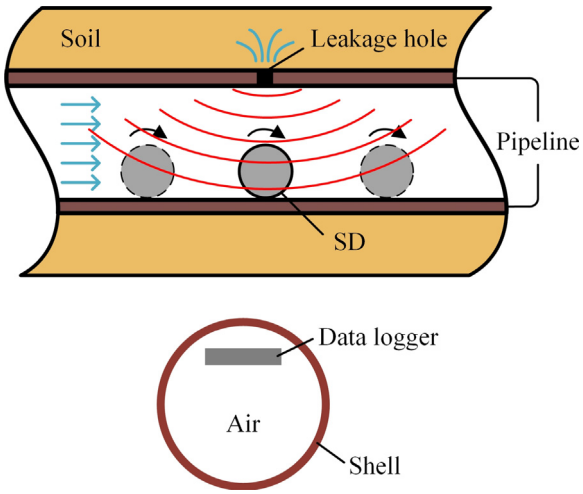

Fig. 1. Leak detection principle of the SD.

2. Characteristics of leak induced sound in the pipe

2.1. Frequency characteristics

A broadband hydrophone was used to test the leak sound signal of the liquid-filled pipe from the inside. The experimental apparatus is shown in Fig. 2. The model number of the hydrophone is TC4013 bought from a Danish company Reson. The diameter of the steel pipe is 219 mm and the length is 12 m. A guide rail was fixed at the bottom of the pipe, and a slider was installed on the guide rail. The hydrophone was fixed on the slider and could move freely along the guide rail by dragging the haulage rope. Water was injected into the pipe from the inlet valve. When the pipe was filled with water, leak occurred from the leak hole. After the pressure in the pipe reached a certain value, the valve was closed to make the leak gradually decrease and stop naturally.

The leak holes used in the experiment are on detachable plugs which are installed on the pipe wall. There are three plugs: with no hole, with a Φ0.6 mm hole in the center, and with a Φ1 mm hole in the center. First, the background noise in the pipe without leak was collected when the plug with no hole was installed on the pipe. Then, the leak sound signals were collected respectively when the other two plugs with holes were installed to generate different leakages. The three groups of recorded leak sound signals and the corresponding spectra are shown in Fig. 3. It can be seen from signals in both time and frequency domains that the sound intensity when leak occurs are noticeably higher than that of the background noise when there is no leak. The larger the leak hole is, the greater the intensity of the leak sound is. It is worth noting that the leak sound signal is broadband covering the frequency range of 100–5000 Hz. This is very important for the design of the SD when considering the acoustic resonance of the air cavity inside the SD. The SD uses the acoustic resonance to focus acoustic energy into a small area where the acoustic sensor locates so as to achieve high acoustic sensitivity, so the SD is narrow-band. It is achievable to design the size of the SD to have its resonance frequencies covered by the broadband leak sound.

2.2. Spatial distribution characteristics

FE simulations were carried out to study the spatial distribution characteristics of the leak induced sound signal in the pipe. 3D simulation model of the water column inside the pipe is shown in Fig. 4(a). The water column is 12 m long with a radius of 100 mm. A monopole point source is set at the midpoint of the water column to mimic the leak sound source. The spatial distribution of acoustic pressure in the pipe obtained by the simulation is shown in Fig. 4(b). The acoustic pressure distribution in the pipe is symmetrical about the sound source. The closer the measurement point is to the sound source, the greater the sound pressure is. The leak sound can cover several meters which are sufficient for the SD to capture the leak sound signals. In other words, when the SD rolls from a distance to approach the leak point, the acoustic signals received by the SD will gradually increase and reach the maximum when the SD is directly below the leak point. It should be pointed out that the average density of the SD is not equal to that of the liquid in the pipe, so the SD will either sink to the bottom of the pipe or float at the top of the pipe. The SD will roll forward along either the top or the bottom of the pipe driven by the fluid. As the SD keeps rotating and moves forward, the incident angle of the leak sound is always changing in the SD's coordinate system, thus the

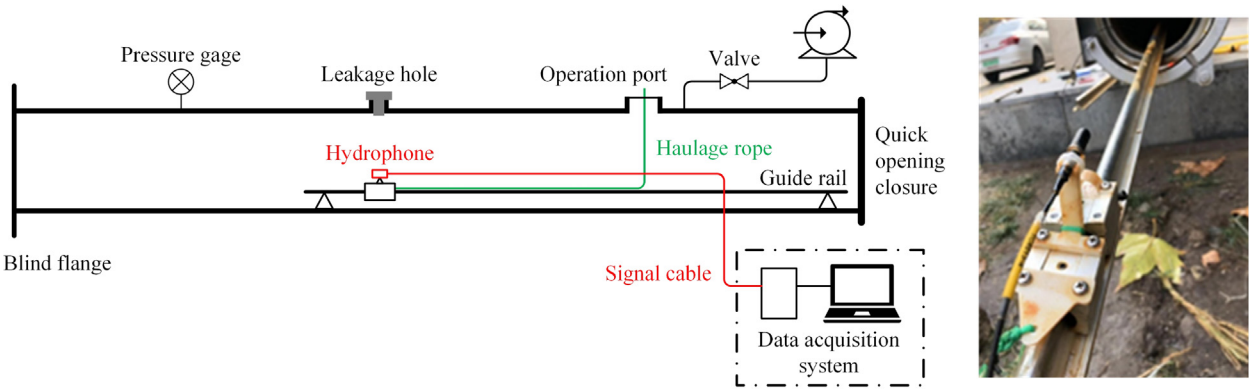

Fig. 2. Experimental apparatus for testing leak-induced sound characteristics.

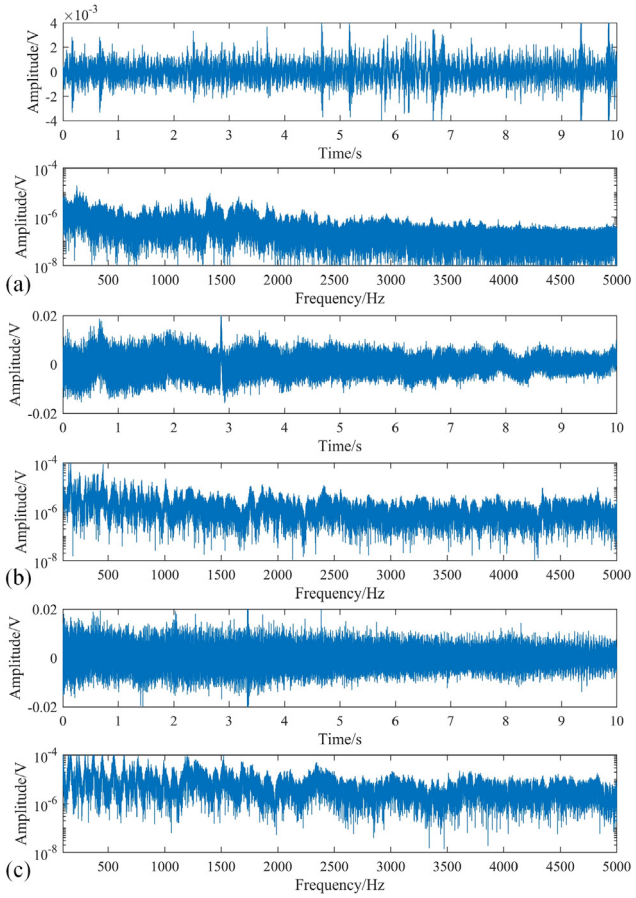

Fig. 3. Background noise and its spectrum with no leak (a); leak sound signals and their spectra with the 0.6 mm leak hole (b) and the 1 mm leak hole (c).

influence of the acoustic sensing directivity of the SD should be considered.

3. Acoustic sensing characteristics of the SD

3.1. Internal acoustic pressure distribution

The SD detects leak sound with a high sensitivity by using the acoustic resonance of the closed air cavity. The data logger is sealed in a closed air cavity to sense and record the acoustic pressure transmitted from the external water to the air cavity. Therefore, the SD is particularly suitable for receiving signals near the resonant frequency of its air cavity. Different resonance frequencies correspond to different acoustic pressure field distributions, that is, different modes. The appropriate mode should be selected to make the SD have higher sensitivity under real operation conditions. The characteristic frequencies and modes of an air cavity with a diameter of 96 mm were calculated via FE simulations. A $35 \times 35 \times 10$ mm^3 block was placed inside the air cavity to mimic the data logger. The sizes of the air cavity and the data logger are the same as those of the actual objects in the subsequent experiments. The characteristic frequencies of the air cavities with and without a data logger were calculated, some of which and the corresponding internal acoustic pressure distributions are shown in Fig. 5.

The first four characteristic frequencies of the air cavity without the data logger are 2368.8 Hz, 3803.3 Hz, 3803.4 Hz and 5113.8 Hz, respectively. The acoustic energy of the first three modes is mainly distributed at the two poles of the sphere, and the fourth is mainly distributed in the center, which is centrosymmetric. When there is a data logger, the 2368.8 Hz and 3803.3 Hz modes still exist stably, but the acoustic energy near the data logger is strengthened; the 3803.4 Hz mode disappears and changes into the 4536.6 Hz mode; the centrosymmetric 5113.8 Hz mode is significantly distorted. Therefore, when the data logger is placed at the edge of the sphere,

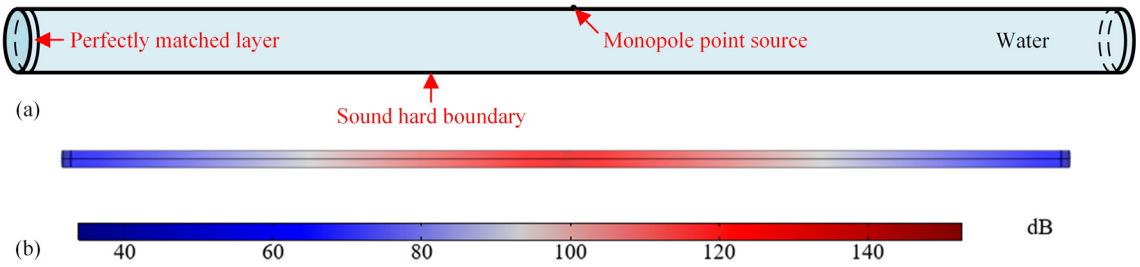

Fig. 4. Simulation model and results of pipeline leak sound distributions.

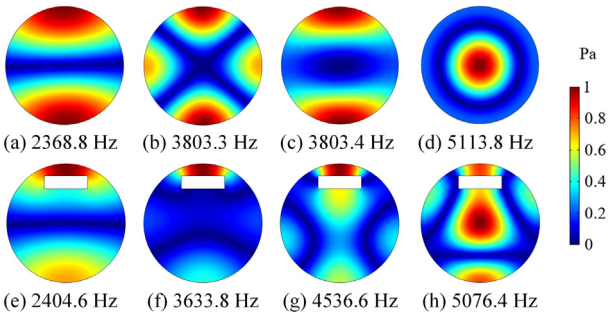

Fig. 5. Acoustic pressure distribution of different characteristic frequencies.

it is much easier for the SD to capture more noticeable acoustic signals and achieve higher sensitivity of small leak detection.

In practical applications, other sensors or batteries may be placed in the SD, which will also affect the sound field distribution in the sphere. This was demonstrated by FE simulations, as shown in Fig. 6. The sound field distributions of the same mode were compared for the cases with and without other electronic parts. It can be seen that although the characteristic frequency has a little deviation, the acoustic pressure at the edge of the SD has little change. Hence, the acoustic pressure of this mode is strong and very stable, and can be used by the SD so as to achieve better response to 2.4 kHz sound signal that is contained in the wideband leak sound. For the centrosymmetric mode, when multiple objects are placed into the SD, the mode disappears, indicating that the mode is unstable.

3.2. Frequency response characteristics

In order to study the frequency response characteristics of the SD, another FE simulation was carried out. The simulation model is shown in Fig. 7(a). A SD was placed in the center of a 300 × 300 × 300 mm^3 water area. The side and bottom surfaces of the water area are set as perfectly matched layer with no acoustic reflection, and the top surface is set as the incident plane. The sound wave transmits into the water with its direction of propagation perpendicular to the incident plane. The inner diameter of the SD is 96 mm and the shell thickness is 3 mm. The SD's geometric dimension is the same as that used in the subsequent experiments. The angle between the data logger axis and the incident wave direction is defined as the directivity angle, and is denoted as θ. When the data logger faces the sound source, θ = 0.

The frequency of the incident acoustic pressure was swept from 1 kHz to 6 kHz to obtain the frequency response curve of the SD. Two measuring points were selected inside the SD, one in the center and the other at the edge, between the data logger and the shell. The frequency response curves measured at the two points are shown in Fig. 7(b). It can be seen that there are noticeable

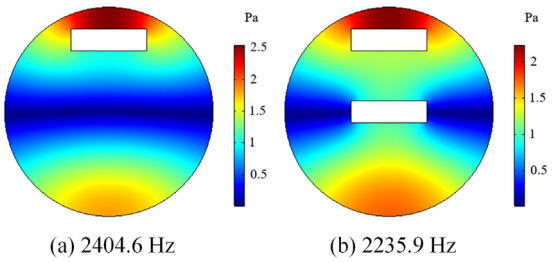

Fig. 6. Acoustic distribution of SDs with different amounts of contents around 2.4 kHz.

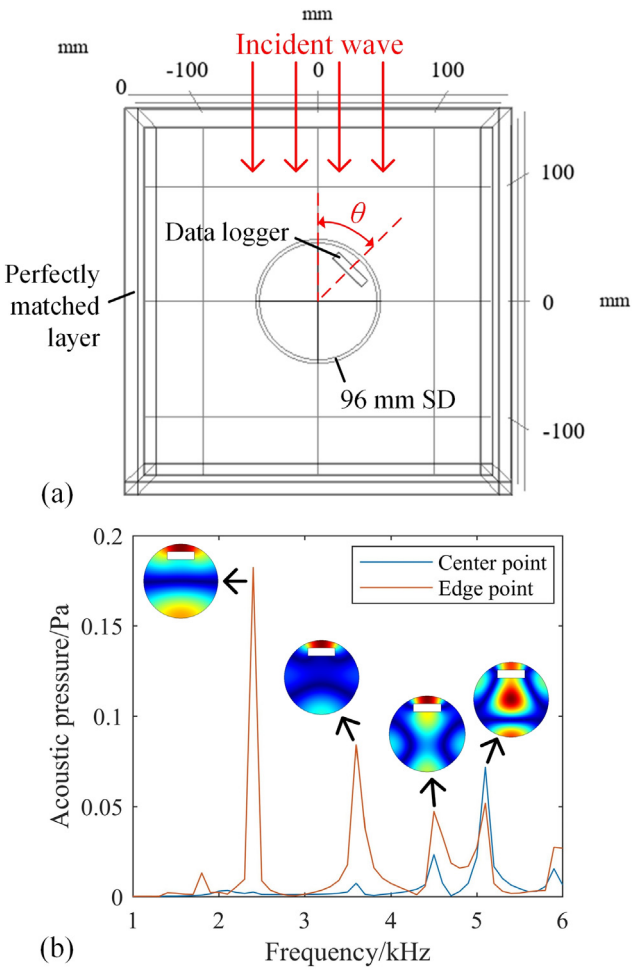

Fig. 7. Frequency response simulation: (a) simulation model; (b) frequency response curves with different acoustic modes.

peaks at 2.4 kHz, 3.6 kHz, 4.5 kHz and 5.1 kHz at the edge point, while the noticeable peaks at the center point appear at 4.5 kHz and 5.1 kHz. The frequencies corresponding to these peaks are in good agreement with the characteristic frequencies of the air cavity as shown in Fig. 5. In Fig. 7(b), acoustic pressure distributions in the sphere corresponding to each characteristic frequency are plotted as subgraphs next to the peaks. Although there is acoustic energy accumulation near the data logger in all modes, the acoustic pressure at the edge of the 2.4 kHz mode is much higher than that of other modes, so it is very suitable for the data logger to be fixed at the edge of the air sphere and collect sound signals using this layout.

3.3. Directivity

The simulation model of directivity test is the same as that of the frequency response test simulation as shown in Fig. 7(a). Two characteristic frequencies of the air cavity, 2404.6 Hz and 5076.4 Hz, were selected to sweep the directivity angle θ of the data logger, and the sweeping range was 0–360°. The measuring points were selected at the edge of the SD, and the acoustic pressure at each angle was normalized by the peak amplitude and plotted in the polar coordinate.

For the 5076.4 Hz mode, the maximum acoustic pressure in the sphere has only one region and is distributed near the center of the sphere; for the mode of 2404.6 Hz, the maximum acoustic pressure in the sphere has two regions, which are distributed in the incident

direction and located at two edges of the air sphere. Therefore, when the incident angle of the sound wave changes, the SD will have no directivity for the former mode, but it will show a certain directivity for the latter. The simulation results shown in Fig. 8 verify this prediction. When the incident wave is 5076.4 Hz, the change of acoustic pressure is relatively small during the SD rotation, and the directivity curve is approximately circular, which indicates that the SD has no directivity at this frequency; when the incident wave is 2404.6 Hz, there are two obvious poles in the directivity curve, and the curve is in the shape of "∞", which indicates that the SD has obvious directivity at this frequency.

3.4. Different shell materials

Three kinds of SDs were manufactured to collect the leak sound signals of a closed water tank, as shown in Fig. 9. Shell materials of the three SDs are photosensitive resin, aluminum, and aluminum covered with polyurethane. There are two purposes of this experiment: (1) to compare the characteristic frequencies of the leak sound signals collected by SDs of different materials; (2) to compare the leak detection sensitivity of SDs of different materials. Before the leak test, the SD was placed in a sealed tank and fixed with weights and ropes. There were two holes on the lid of the sealed tank: one was the water inlet hole, which was connected to the tap water with the pressure of 0.3 MPa, and the water was continuously injected into the sealed tank through the hole; the other was a leak hole with a diameter of 3 mm, where the extra water flowed out and leak occurred. During the experiment, the tank was placed horizontally. The location of the SD in the sealed tank is shown in the subgraph of Fig. 9. The experimental process was as follows: put the SD into the tank, seal up the tank with the lid, fill it with water after sealing, start timing when leak occurs, close the water inlet valve, wait for 30–60 s until the leak hole no longer leaks and stop the test, open the sealed tank, take out the SD and download the data.

Original data, time-frequency diagram and some details of the leak sounds in time and frequency domains, recorded by three kinds of SDs, are shown in Fig. 8. The left, middle and right columns are the signals recorded by the photosensitive resin SD, aluminum SD, and aluminum & polyurethane SD, respectively. The inlet valve is closed at about 1 s. The sharp increase of the acoustic signal at

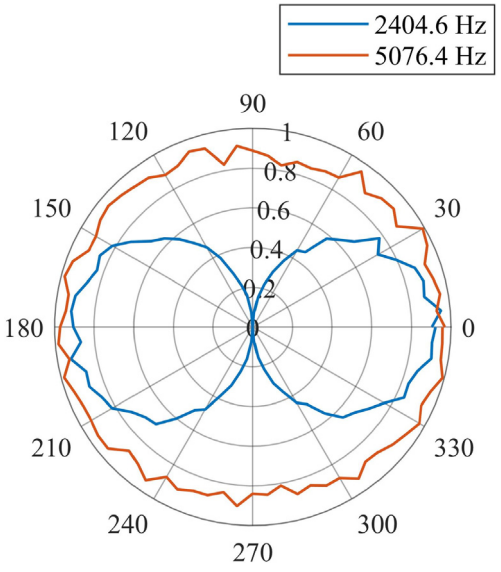

Fig. 8. Directivity simulation results of the SD with different acoustic modes.

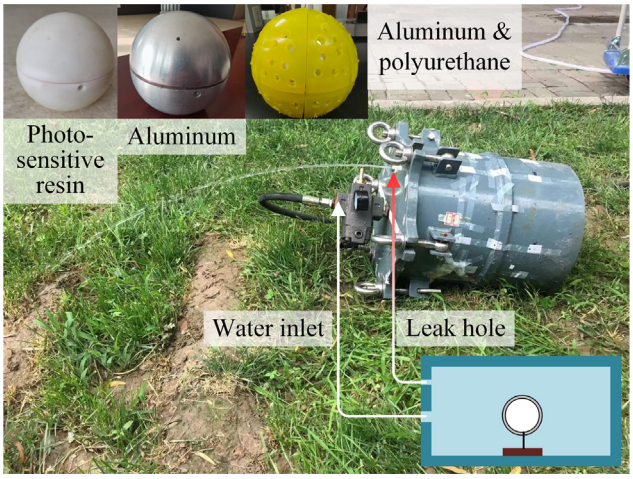

Fig. 9. Leak test apparatus with a pressurized water-filled tank.

1 s is due to the noise produced by backflow when the valve is suddenly turned off. The first 1 s of the original signal indicates that water is being injected into the sealed tank, and after 1 s, it indicates that water injection has been stopped and the leak continues to weaken until it stops. In the short-time Fourier spectrum shown in Fig. 10(b), (d) and (f), the signal is relatively strong, and its intensity remains unchanged within 1 s. After 1 s, the intensity gradually weakens until it finally disappears. As time goes by, the leak flow becomes smaller and smaller, and the corresponding leak signal is also smaller, which conforms to the fact that the leak is weakening. It is also proved that all the three SDs can detect the sound signal of the leak. The first characteristic peaks of the spectra of the three SDs all exist and are almost identical. The signal intensity of the photosensitive resin SD is stronger when compared with the other two SDs, so more characteristic frequencies can be detected. The characteristic frequencies of the leak signals collected by the three SDs are marked in the subgraphs of Fig. 10(a), (c) and (e), and the first peaks in each subgraph are very close to the characteristic frequency 2404.6 Hz of the first mode as shown in the characteristic frequency simulation section. Therefore, the characteristic frequency is determined by the resonance mode of the air cavity in the air sphere, and is independent of the shell. Moreover, the first characteristic peak splits into two, which is due to the addition of data logger and the slight change of the symmetry of the spherical air cavity by the internal combination structure, and the frequencies with the same mode in different directions are no longer the same.

The photosensitive resin SD may be not so pressure-resistant as the aluminum SD or the aluminum & polyurethane SD. The former can be used for low-pressure pipelines, while the latter two are suitable for detecting leak in high-pressure pipelines. A polyurethane coating on the aluminum SD can reduce vibration and enhance wear resistance. In the three measurements, the conditions of leak generation and extinction are identical, so the acoustic pressure of the leak signal is also identical. The experimental results show that the characteristic frequencies of the leak sound signals collected by the three SDs are the same, but the signal amplitudes are obviously different. The amplitudes of the leak signals received by the SD are 0.03 V, 0.012 V and 0.003 V respectively at 0.5 s after stopping water injection. The signal amplitude of the photosensitive resin SD is 2.5 times as large as that of the aluminum SD and 10 times of the aluminum & polyurethane SD. This indicates that the photosensitive resin shell has the best sound permeability and its sensitivity is the highest.

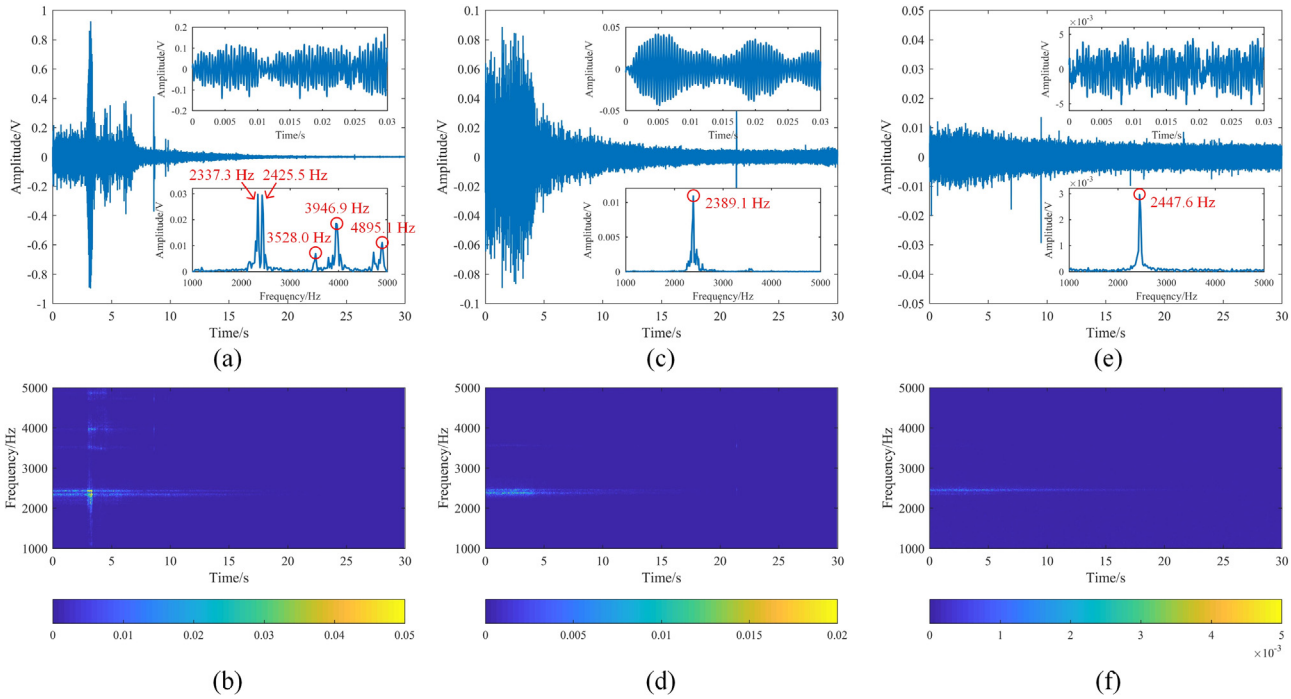

Fig. 10. Leak signals detected by three different SDs: (a and b), by the photosensitive resin SD; (c and d), by the aluminum SD; (e and f), by the aluminum & polyurethane SD.

4. Pipeline leak detection test

Leak detection test was carried out on a 12 m long, DN200 steel pipeline, as shown in Fig. 11. The SD was placed near the leak point. The pipe was filled with water and pressurized to 0.3 MPa. When the pipe began to stably leak, the water inlet valve was closed. The pipe continued to leak, but the leak rate gradually decreased as the pressure decreased. The SD collected the leak-caused acoustic signal during the entire process of leak test. After the leak stopped, the SD was taken out from the pipe and the data was downloaded for spectrum analysis. During the leak detection test, a plastic basin was placed on an electronic scale, and they were placed in front of the leak hole to pick up the falling leaked water. The pressure in the pipe and the mass of the leaked water were continuously recorded. The differential of the leak quantity with respect to time was calculated to obtain the instantaneous leak rate.

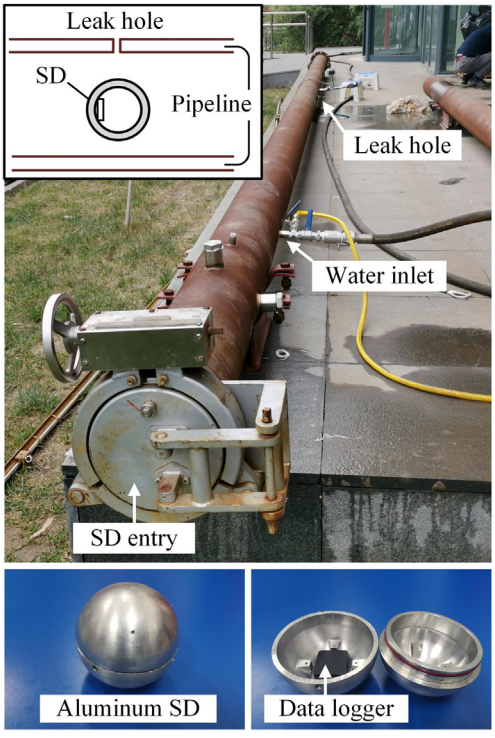

Fig. 11. Leak detection experiment for a water-filled pipeline using the proposed SD.

As can be seen in Fig. 12(a) that after the water inlet valve is closed, the leak lasts for about 9 min. During this process, the average amplitude of the leak signal near the characteristic frequency (2200–2400 Hz) becomes smaller and smaller. The pressure in the pipe dropped from 300 kPa to 23 kPa and the leak rate dropped from 7 g/s to 2 g/s, as shown in Fig. 12(b). After the water inlet valve is closed, the amplitude of the leak signal decreases rapidly first, then slowly, and finally approaches a fixed value, which means that the characteristic component at the resonance frequency does no longer indicate the leak. Time-frequency spectrograms of the leak sound during three different time periods are displayed in Fig. 12(c), and they clearly indicate that the main component of the leak sound is gradually weakening. The characteristic peak of the spectrogram does not change after 280 s, and it is caused by the background noise. The spectrum curves of the leak signal near 0 s, 70 s and 280 s are shown in Fig. 12(d). It can be seen that the leak signal cannot be detected after 280 s. At this time, the pressure was 70 kPa and the leak rate was 2.72 g/s, namely, 0.164 L/min which is the leak detection threshold.

The proposed SD has a very high leak detection sensitivity. In ref. [14], a MEMS hydrophone is used inside the pipe and the leak rate is 30 L/min. In Ref. [15], piezoelectric accelerometer and hydrophone are used outside and inside the pipe, and the smallest leak rate is 180 L/h (=3 L/min). In Ref. [16], accelerometers are used outside the pipe and the smallest leak rate is 2.1 L/min. In Ref. [17], FBG based temperature sensors are used outside the pipe and the

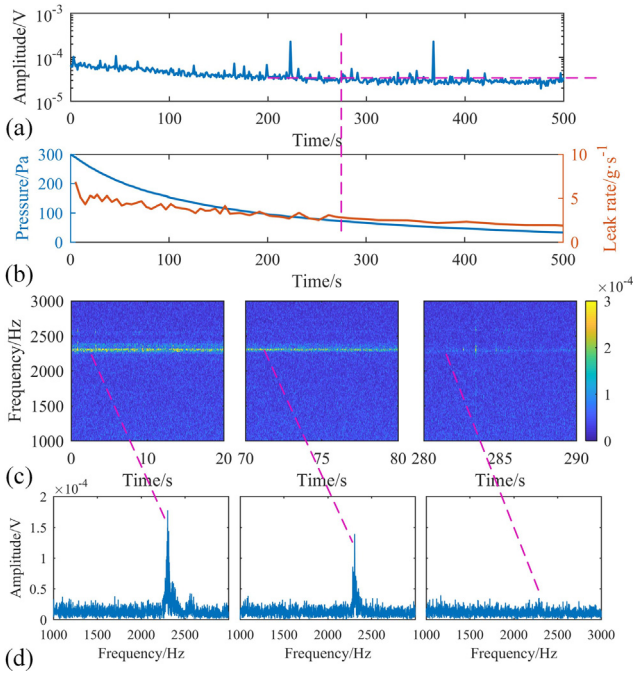

Fig. 12. Leak detection results: (a) average amplitude near the characteristic frequency while the leak becomes weaker and weaker after the water inlet valve is closed; (b) pressure and leak rate tendency during the leak detection experiment; (c) time-frequency spectrograms of the leak sound during three different time periods; (d) spectrum curves of the leak sound at three different moments.

smallest leak rate is 2.3 mL/s (=0.138 L/min), which is the most sensitive. Leak detection threshold of the proposed SD is 0.164 L/min which is a very high leak detection sensitivity.

5. Discussions

The SD diameter should be customized according to the pipeline diameter. Outer diameter of the detector for a pipeline with a large diameter should be enlarged in order to obtain sufficient thrust force from the internal fluid, so that the detector can easily pass through some upward pipe sections. When the outer diameter is enlarged, the inner diameter should also be enlarged to reduce the detector weight to achieve reliable passability and restrict the shell thickness to achieve good sound permeability. Enlarging the inner diameter will reduce the resonance frequency, but this does not affect leak detection performance, because the leak-induced acoustic signals are broadband and have higher amplitude in lower frequency range.

Locating the data logger on one side of the cavity can use the mode with a "∞" directivity as shown in Fig. 8, and locating the data logger in the center can use the mode that is omnidirectional. However, it is more convenient to fix the data logger on the side in practical application, and it has been proved that the omnidirectional model is unstable, so the mode with a "∞" directivity is used by the spherical leak detector. For leak detection of a field pipeline, the detector is rolling forward under the impetus of the internal flow. Sometimes the leak point may be at the shaded area of the detector's directivity, but this is temporary, because the detector can roll over several cycles while passing by the leak point and the leak sound can cover several meters.

6. Conclusions

Via FE simulations and experiments, this paper investigates the acoustic sensing characteristics of the internal SD for tiny, continuous leak detection of liquid-filled pipelines, and demonstrates its high leak detection sensitivity. Both the detection principle and working conditions of the SD are taken into account. The following conclusions can be obtained:

(1) The original leak sound signal is broadband, and the acoustic pressure in the pipe can cover several meters, so the acoustically resonant, narrow-band and movable SD can always capture the leak signal. The SD forms a closed air cavity which may acoustically resonate and thus amplify the transmitted sound induced by leaks.
(2) The SD has multiple resonant frequencies each of which corresponds to a different acoustic pressure distribution mode and directivity. Among them, the first mode is most stable and hardly affected by electronic parts in the SD that may slightly change the air cavity. The acoustic directivity does not hinder leak detection, because the SD will roll over several cycles while passing by the leak point.
(3) Characteristic frequencies of the SD are determined by the air cavity and independent of shell materials; nevertheless, the resin SD has better sound permeability than the aluminum SD, and therefore has higher sensitivity. Finally, the aluminum SD is used to detect the leak in a water-filled pipeline and achieves a high sensitivity up to 0.164 L/min.

Declaration of Competing Interest

The authors declare that they have no known competing financial interests or personal relationships that could have appeared to influence the work reported in this paper.

Acknowledgements

This work is supported by National Natural Science Foundation of China (Nos. 61803280, 61973227).

References

[1] Mohd Ismail MI, Dziyauddin RA, Ahmad Salleh NA, Muhammad-Sukki F, Aini Bani N, Mohd Izhar MA, et al. A review of vibration detection methods using accelerometer sensors for water pipeline leakage. IEEE Access 2019;7:51965–81.
[2] Zaman Dina, Tiwari Manoj Kumar, Gupta Ashok Kumar, Sen Dhrubjyoti. A review of leakage detection strategies for pressurised pipeline in steady-state. Engineering Failure Analysis, vol. 109; 2020.
[3] Shama AM, El-Rashid A, El-Shaib M, Mohamed Kotb D. Review of leakage detection methods for subsea pipeline. Maritime Trans Harvest Sea Resour 2018;2:1141–49.
[4] Chun-hua T, Jun-chi Y, Jin H, Yu W, Dong-Sup K, Tongnyoul Y. Negative pressure wave based pipeline leak detection: challenges and algorithms. In: Proceedings of 2012 IEEE international conference on service operations and logistics and informatics, 8-10 July 2012, Piscataway, NJ, USA. p. 376–80.
[5] Reynolds Joe, Kam Amy. An evaluation of negative pressure wave leak detection: challenges, limitations, and use cases. In: PSIG Annual meeting, PSIG; 2019.
[6] Papastefanou AS, Joseph PF, Brennan MJ. Experimental investigation into the characteristics of in-pipe leak noise in plastic water filled pipes. Acta Acustica United Acustica 2012;98(6):847–56.
[7] Muggleton JM, Brennan MJ, Pinnington RJ. Wavenumber prediction of waves in buried pipes for water leak detection. J Sound Vib 2003;249(5):939–54.
[8] Liu C, Li Y, Fang L, Xu M. Experimental study on a de-noising system for gas and oil pipelines based on an acoustic leak detection and location method. Int J Press Vessels Pip 2017;151:20–34.
[9] Liu J, Li T, Liu T, Li Q. The attenuation characteristics of waves in fluid-filled pipes surrounded by elastic media. J f Huazhong Univ Sci Technol 2003;31(10):90–2.
[10] Hunaidi O, Chu WT. Acoustical characteristics of leak signals in plastic water distribution pipes. Appl Acoust 1999;58(3):235–54.
[11] Xu T, Chen S, Guo S, Huang X, Li J, Zeng Z. A small leakage detection approach for oil pipeline using an inner spherical ball. Process Saf Environ Prot 2019;124:279–89.

[12] Kumar D, Dezhan T, Naifu Z, Shah RA, Dibo H, Hongjian Z. The free-swimming device leakage detection in plastic water-filled pipes through tuning the wavelet transform to the underwater acoustic signals. Water 2017;9(10):731.
[13] Fletcher Richard, Muthu Chandrasekaran. SmartBall™-a new approach in pipeline leak detection. In: Proceedings of the Biennial international pipeline conference, IPC, vol. 2; 2009. p. 117–33.
[14] Xu Jinghui, Chai Kevin Tshun-Chuan, Wu Guoqiang, Han Beibei, Wai Eva Leong-Ching, Li Wei, et al. Low-cost, tiny-sized MEMS hydrophone sensor for water pipeline leak detection. IEEE Trans Ind Electron 2019;66(8):6374–82.
[15] Alberto Martini, Marco Troncossi, Alessandro Rivola. Vibroacoustic measurements for detecting water leaks in buried small-diameter plastic pipes. J Pipeline Syst Eng Pract 2017;8(4):04017022.
[16] Yazdekhasti Sepideh, Piratla Kalyan R, Atamturktur Sez, Khan Abdul. Experimental evaluation of a vibration-based leak detection technique for water pipelines. Struct Infrastruct Eng 2018;14(1):46–55.
[17] Willem Jacobsz Schalk, Ingo Jahnke Sebastian. Leak detection on water pipelines in unsaturated ground by discrete fibre optic sensing. Struct Health Monitor 2019. https://doi.org/10.1177/1475921719881979.